Eur. Phys. J. A **6**, 303–308 (1999)

THE EUROPEAN PHYSICAL JOURNAL A

Resonance strength measurements of the ^{27}Al(p,γ)^{28}Si reaction in the energy range $E_p = 0.8 - 2.0$ MeV

C. Chronidou, K. Spyrou, S. Harissopulos, S. Kossionides, T. Paradellis

N.C.S.R. "Demokritos", Institute of Nuclear Physics, Laboratory for Material Analysis, Aghia Paraskevi Attikis 153 10, Athens, Greece

Received: 21 June 1999 / Revised version: 6 August 1999
Communicated by D. Schwalm

Abstract. An excitation function of the ^{27}Al(p,γ)^{28}Si reaction has been measured over the proton beam energy range E_p=800-2000 keV using a 4π NaI segmented crystal. In the above energy range 47 narrow resonances were measured and their strengths have been deduced. The absolute efficiency of the detection system has been determined for each one of the resonances via Monte-Carlo simulation, taking into account the decay scheme of each resonance. The results of the present work are compared with literature.

1 Introduction

The ^{27}Al(p,γ)^{28}Si reaction plays a significant role in stellar nucleosynthesis as it is one of the reactions that form the Mg-Al cycle. The Mg-Al cycle is present mainly during hydrogen burning in second generation stars for T_9 $\geq$0.03. The ^{27}Al(p,γ)^{28}Si reaction is the leakage reaction of the cycle as it destroys the catalytic material and competes with the ^{27}Al(p,α)^{24}Mg reaction which provides the return flow to the cycle. Although many measurements of the resonances of the ^{27}Al(p,γ)^{28}Si reaction have been reported in literature, the results for the resonance strengths cover a wide range of values, due to the fact that the measurements have been carried out with various detection systems and the results been deduced with different analytic techniques and methods of analysis. Therefore, many uncertainties and large discrepancies are still present [1]. In the present work all 47 resonances of the ^{27}Al(p,γ)^{28}Si reaction present in the energy range E_p=0.8-2.0 MeV have been measured using a 4π NaI summing detector. The absolute efficiency of the detection system was determined via Monte-Carlo calculations in which the decay scheme of each one of the resonances has been taken into account. The results of the calculations have been validated with the use of three different nuclear reactions. The great advantages of the specific detection system, i.e. the large solid angle -that approaches 4π- covered by the detector and the fact that the measurements are angle integrated, lead to valid and self-compatible results.

2 Experimental setup and procedures

All measurements have been carried out in the Tandem Laboratory of the Institute of Nuclear Physics of N.C.S.R. Demokritos, Athens, using the 5.5 MV Tandem-Van de Graaff accelerator. The proton beam energy varied from 800-2000 keV while the energy step in most of the range was 1 keV. The total charge collected on the target varied from 10 -120 μCb. Typical currents used were I_p=50-600 nA, limited by dead time, that was kept below 10% during the whole set of measurements. The accelerator was energetically calibrated using the well known energy of the E_R=991.86 keV narrow resonance of the ^{27}Al(p,γ)^{28}Si reaction. The proton beam energy spread was found to be Δ_b=1.6$\pm$0.2 keV at E_p=1.0 MeV. The targets used during the whole set of measurements were produced by evaporation of pure metallic aluminium (99.9999%) on clean Cu and W backings. In each evaporation, close to the W and Cu backing a 2 mg/cm^2 gold foil was placed. These foils were used to determine the O and C present in the targets by alpha RBS analysis at E_α=3.06 MeV. In all cases the O/Al and C/Al atomic ratios were less than 0.006. All targets were free of Fluorine as determined by using the ^{19}F(p,$\alpha\gamma$) resonance at E_p=872 keV. The target on the Cu backing was used for E_p $\leq$1100 keV while the targets on the W backing were used for E_p $\geq$1100 keV. The thickness of all the targets was determined via thick target yield measurements of narrow resonances of the ^{27}Al(p,γ)^{28}Si reaction. The thickness of the target on the Cu backing was determined using the well known [1] narrow resonance at E_R=992 keV and was found to be Δ_t=46.5$\pm$2.3 $\mu g/cm^2$. The thicknesses of the two targets on W backing were determined using the narrow resonances at 992, 1025, 1262 and 1587 keV and were found to be Δ_t=43.0$\pm$1.3 μg/cm^2 and Δ_t=41.4$\pm$1.5 μg/cm^2 respectively. The thickness of these targets corresponds to an energy loss Δ_{lab} of about 7.5 keV at E_p=992 keV. Finally, a thicker target on W backing was used for thick target measurements of some resonances. The thickness of

that target was determined via measurements of the resonances at E_R=1025, 1118, and 1262 keV and was found to be Δ_t=65.3±1.9 μg/cm^2 corresponding to an energy thickness of about 11.5 keV at E_p=992 keV. Targets were frequently checked for deterioration via measurements of the E_R=991.86 keV resonance of the ^{27}Al(p,γ)^{28}Si reaction and were found to be stable within 5%. The detection system used during the whole experiment is a 4π NaI(Tl) summing detector which has been described in detail previously [2]. A schematic diagram of the detection system is shown in Fig. 1a. The beam collimating system is shown in Fig. 1b. The proton beam passes through two apertures (6 mm and 3 mm diameter respectively) and is focused onto a spot of about 4 mm diameter on the target. The target is placed at the end of a stainless steel tube at a distance of 100 cm from the first collimator. The second collimator is placed 40 cm away from the target. A PVC cylinder is placed at a distance of 5 cm from the end of the tube to isolate the target holder which can be mechanically mounted on the end of the target tube by tightening a hollow brass cylinder. A lead ring of about 1 mm thickness was used as a vacuum sealing material between the target holder and the tube, while the rest of the beam line is sealed with copper gaskets. The beam line includes 3 cooling traps and 4 turbo pumps. The last pump is located at the beginning of the tube before the first collimator, at a distance of about 120 cm from the target position. With the setup described above, a vacuum of 3×10^{-8} Torr has been achieved. The target holder served as a Faraday cup for current integration. A voltage of -300V was applied to the other part of the beam tube for suppression of the secondary electrons. The NaI detector is fixed on an iron frame that can be moved on a railway. Thus, the target holder can be placed at the center of the detector. The absolute efficiency of this detection system has been determined by calculations with Monte-Carlo simulation, based on the GEANT package [3]. The validity of the calculations was checked experimentally with three nuclear reactions [2], yielding agreement to within 6%. Therefore, absolute efficiencies from the Monte-Carlo simulation, can be used faithfully for the rest of the analysis. Due to the fact that the final signal is the sum of all the γ-rays emitted, the absolute efficiency depends strongly on the multiplicity and/or the energy of the photons detected. In the case of the ^{27}Al(p,γ)^{28}Si reaction, the absolute efficiency was calculated for each resonance separately taking into account the specific decay scheme of each resonance. An example of such calculation is given below for the 992 keV resonance. The compound nucleus, ^{28}Si, deexcitates to the ground state via 15 different decay modes [4], which are displayed in Fig. 2. The branching ratios for each decay mode and the gamma ray branching ratios of the levels of ^{28}Si have been taken from literature [4], [5] and are accompanied by a mean error of 5%. For each one of the decay modes the absolute efficiency was calculated using Monte-Carlo simulation. In Table 1, the decay modes, the branching ratios and the corresponding absolute efficiency calculated for an 8-15 MeV window of integration, are listed. An overall absolute efficiency ϵ is finally quoted which is the linear

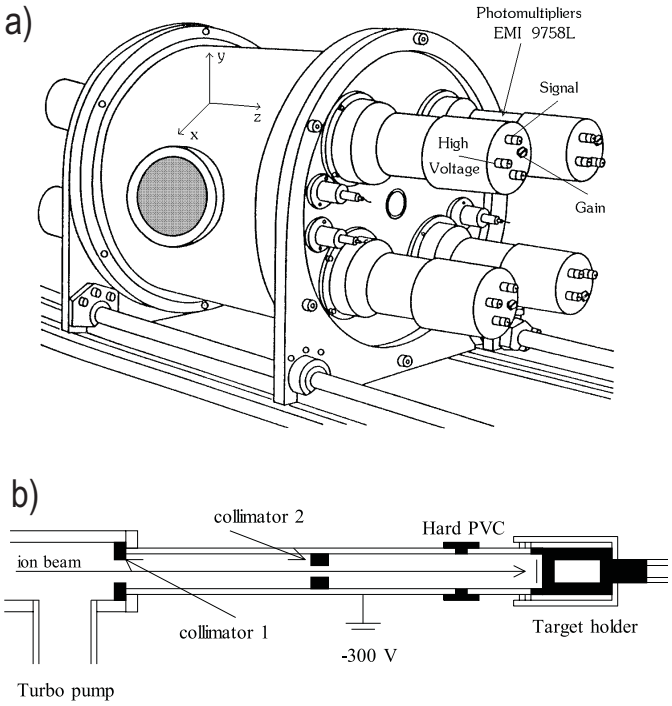

Fig. 1. Schematic diagram of the experimental setup a) Detection system, for details see [2]. b) Beam collimating and target system

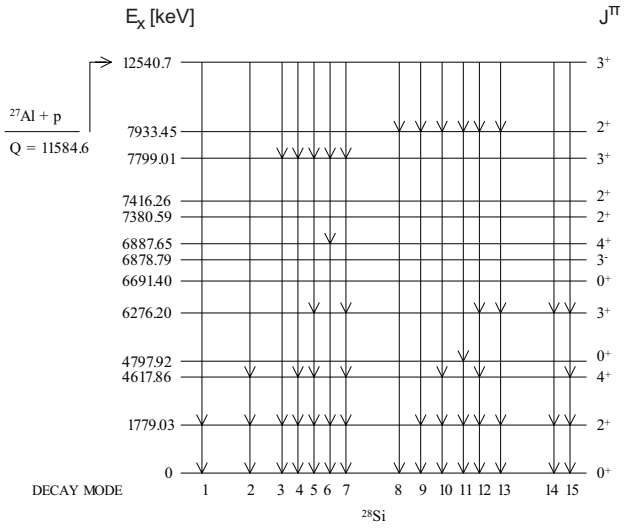

Fig. 2. Decay modes of the 992 keV resonance

combination of the absolute efficiency for each decay mode times the corresponding branching ratio. The uncertainty is 8%. The overall efficiencies applicable to another 47 resonances of interest have been calculated with branching ratios adopted from [4]-[11]. The results are given in Table 2 further below.

An excitation function of the ^{27}Al(p,γ)^{28}Si reaction in the energy range E_p=800-2000 keV is displayed in Fig. 3,

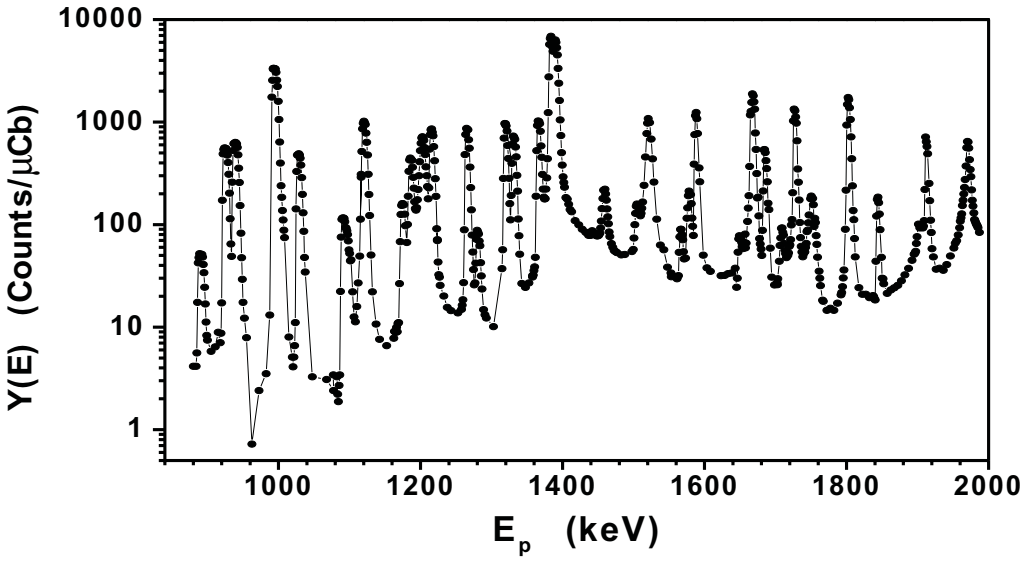

Fig. 3. Excitation function of the ^{27}Al(p,γ)^{28}Si reaction in the enegy range E_p=800-2000 keV. The solid line is to guide the eye

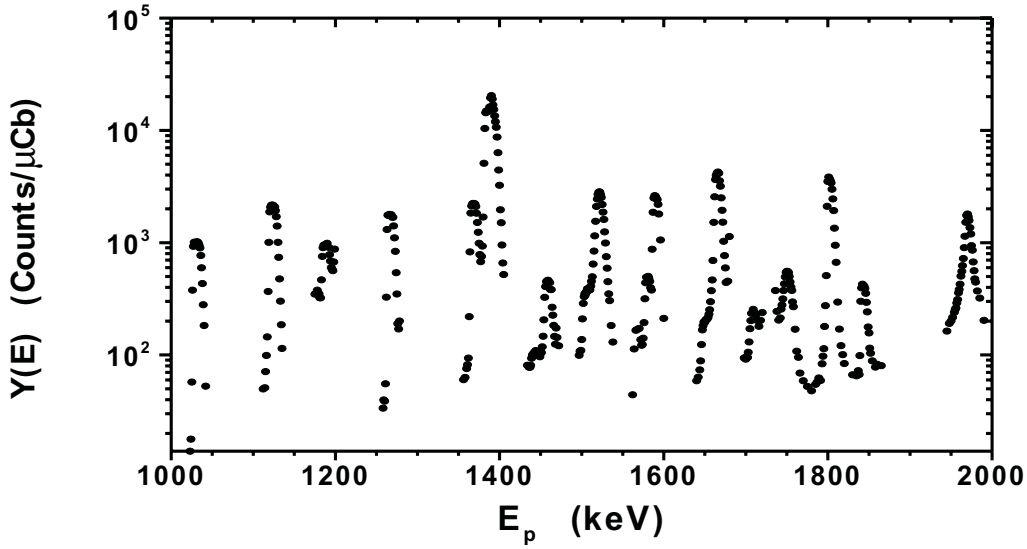

Fig. 4. Excitation function of the ^{27}Al(p,γ)^{28}Si reaction with a thicker W backed target

where more than 850 points are plotted. The targets used were of similar thicknesses, between 41.4 and 46.5 μg/cm^2. Another excitation function with a thicker W backed target (65.3 μg/cm^2) is displayed in Fig. 4, where more than 450 points are plotted. That target was used for thick target measurements for some selected resonances. In both cases, measurements of the Cu and W backings were performed, and the contribution of the backing material to the observed yield has been subtracted. Consequently, the yield plotted in Figs. 3 and 4 stands for the net yield arising from the ^{27}Al(p,γ)^{28}Si reaction.

3 Analysis and Results

The deduction of resonance strengths $\omega\gamma$ has been carried out with two different methods. The first method uses the thick target yield and applies if the existence of a plateau in the excitation function is undoubtful. In that case the resonance strength $\omega\gamma$ is calculated directly from the maximum observed yield at the plateau of the excitation function via the following analytical relation :

$$Y_\infty = N^* \cdot \varepsilon \cdot \frac{\lambda^2}{2}\omega\gamma\frac{M+m}{M}\frac{1}{T(E)} \qquad (1)$$

where T(E) the stopping power of the target, ε the efficiency, N^*=N_A/A, N_A the Avogadro number, and A the

Table 1. Branching ratios and efficiencies for the decays of Fig. 2

Decay mode	Branching ratio %	Efficiency
1	76.4	0.512
2	4.09	0.422
3	5.601	0.321
4	0.1122	0.312
5	2.439	0.312
6	0.0119	0.304
7	0.3272	0.319
8	3.295	0.366
9	0.2178	0.324
10	0.1861	0.304
11	0.1584	0.303
12	0.0111	0.316
13	0.084	0.307
14	1.8963	0.348
15	0.2537	0.380
		ε=0.48

atomic weight of aluminum. The second method has been applied to "thin" target measurements. Although the majority of the resonances of the ^{27}Al(p,γ)^{28}Si reaction in the energy range E$_p$=800-2000 keV have a very small width (varying from several eV up to several hundreds eV) compared to the target thickness ($\sim$7.5 keV at E$_p$=1 MeV), the beam energy spread which was determined to be 1.6 keV at E$_p$=1 MeV and the fact that many resonances, although narrow, are very close to each other, are two factors that do not always allow for thick target measurements. In that case, the reaction yield per incident projectile is given by the equation:

$$dY(E) = N^* \cdot \varepsilon \cdot \sigma \cdot dx \tag{2}$$

where σ the cross section in cm^2, x the infinitesimal target thickness in μgr/cm^2. For a finite target thickness x, the reaction yield becomes an integral of the cross section over the target thickness:

$$Y(E_p) = \varepsilon \cdot N^* \cdot \int_0^x \sigma(E) \cdot dx = \varepsilon \cdot N^* \cdot \int_{E_p - \Delta_{lab}}^{E_p} \frac{\sigma(E)}{T(E)} dE \tag{3}$$

The cross section of an isolated resonance is given by the Breit-Wigner formula:

$$\sigma(E) = \sigma(E_R) \cdot \frac{E_R}{E} \cdot \frac{\Gamma_a(E)}{\Gamma_a(E_R)} \cdot \frac{\Gamma_b(E)}{\Gamma_b(E_R)} \cdot \frac{(\Gamma_R/2)^2}{(E - E_R)^2 + (\Gamma/2)^2} \tag{4}$$

where Γ_a, Γ_b the partial widths for the entrance and the decay channel, and Γ the total width. In our case, $\frac{\Gamma_a(E)}{\Gamma_a(E_R)} = \left(\frac{E_R}{E}\right)^{1/2} \cdot \frac{P_l(E)}{P_l(E_R)}$ where P$_l$(E) the penetration factor and $\frac{\Gamma_b(E)}{\Gamma_b(E_R)} = \left(\frac{E_\gamma}{E_{\gamma,E_R}}\right)^3$ where E$_\gamma$ = $E_{p,cm}$+Q.

In the present work the stopping power values are obtained from Andersen and Ziegler [13]. Two phenomena influence the reaction yield and they have been taken into account, that is the beam energy distribution and the energy straggling of protons inside the target. The first phenomenon has been described with a gaussian distribution of beam energy $g(E, E_p)$ around a mean value E_p. This gaussian function modifies the cross section $\sigma(E)$. The second phenomenon, the spreading of beam energy which accompanies the slowing down of protons inside the target, has also been described with a gaussian distribution around a mean value $E_p - \Delta_{lab}$ at a depth x inside the target. The standard deviation of this straggling distribution is described sufficiently well by Bohr's formula [12]:

$$\Omega_B = \left(0.156 \cdot z^2 \cdot \frac{Z}{A} \cdot x\right)^{1/2} (keV) \tag{5}$$

with x the target thickness in μg/cm^2, Z, A the atomic number and weight of the target, and z the atomic number of the projectile. The total spreading width is the result of contributions from straggling and from the intrinsic energy spread of the beam Δ_b. Both effects have been included in a single gaussian function [14] in order to avoid a triple integral and to simplify the calculations, namely

$$g(E_p, E', x) = B \cdot exp\left[-\frac{(E_p - E' - T(E_p) \cdot x)^2}{0.36 \cdot \Gamma_t}\right] \tag{6}$$

where B is the normalization constant and Γ_t is the total FWHM of the energy spreading:

$$\Gamma_t = \left(\Delta_b^2 + 0.86 \cdot z^2 \cdot \frac{Z}{A} \cdot x\right)^{1/2} \tag{7}$$

Consequently, the reduced reaction yield is given by the double integral :

$$Y(E_p) = \sigma_R \cdot \varepsilon \cdot N^* \cdot \int_0^x \int_0^\infty \frac{E_R}{E'} \cdot \frac{\Gamma_R^2}{4 \cdot (E' - E_R)^2 + \Gamma_R^2} \cdot \cdot g(E_p, E', x) \cdot dE' \cdot dx \tag{8}$$

or $Y(E_p) = \sigma_R \cdot N^* \cdot x_{eff}(E_p; \Gamma_R, E_R, x)$.

Therefore the experimental resonant yield can be fitted using the above expression, for the determination of the cross section σ_R, where the parameters Γ_R and E$_R$ have been taken from literature [5]. In cases where more than a single resonance contribute to the experimentally measured reaction yield, the fit function (8) is slightly modified:

$$Y(E_p) = N^* \cdot \varepsilon_1 \cdot \sigma_{R,1} \cdot x_{eff,1} + N^* \cdot \varepsilon_2 \cdot \sigma_{R,2} \cdot x_{eff,2} + ... \tag{9}$$

An example of fitting procedure is given below for the four resonances at E$_R$ = 1171, 1183, 1200, and 1213 keV. Because of the large width of the 1200 keV resonance (Γ_R=5.4 keV) the values of the σ_R can be deduced only by the fitting procedure. In Fig. 5 the excitation function and the result of the fit for the above mentioned resonances is displayed. Finally from σ_R one can calculate the resonance strength $\omega\gamma$ via the relation:

$$\omega\gamma = \sigma_R \cdot \Gamma_R \cdot \frac{\pi}{\lambda^2} \tag{10}$$

Table 2. Resonance strengths of the ^{27}Al(p,γ)^{28}Si reaction

E_R(keV)(lab)	Efficiency (±8%)	$\omega\gamma$(eV) present	$\omega\gamma$(eV) [1]	E_R(keV)(lab)	Efficiency (±8%)	$\omega\gamma$(eV) present	$\omega\gamma$(eV) [1]
887.78±0.05	0.491	0.012±0.001	0.015±0.002	1564.98±0.08	0.392	0.035±0.008	0.02±0.01
922.96±0.05	0.508	0.140±0.013	0.140±0.018	1577.60±0.08	0.461	0.204±0.022 (2)	0.06±0.02 (2)
937.25±0.03	0.441	0.183±0.017	0.176±0.021	1577.82±0.19	0.461		
991.86±0.03	0.482	1.94±0.07	1.90±0.10	1587.49±0.08	0.472	0.81±0.13	0.78±0.07
1025.29±0.05	0.387	0.35±0.03	0.31±0.03	1647.11±0.08	0.433	0.038±0.011	0.03±0.01
1089.74±0.06	0.419	0.080±0.023	0.08±0.01	1663.0±0.5	0.521	1.58±0.23	1.00±0.18 (2)
1097.26±0.06	0.349	0.043±0.012	0.04±0.01	1664.4±0.2	0.521	0.071±0.012	
1118.63±0.06	0.362	0.80±0.06	0.73±0.13	1679.58±0.10	0.522	0.33±0.09	0.25±0.04
1171.84±0.06	0.479	0.093±0.027	0.071±0.002	1683.57±0.13	0.505	0.011±0.003	0.04±0.03
1183.44±0.08	0.510	0.26±0.04	0.16±0.04	1705.6±0.5	0.439	0.057±0.004	0.04±0.01
1200.4±0.5	0.390	1.02±0.14	0.25±0.10	1723.4±0.6	0.431	0.088±0.014	
1213.08±0.06	0.483	0.49±0.14	0.40±0.04	1724.3±0.6	0.431	1.0±0.3	0.78±0.11 (2)
1262.75±0.07	0.422	0.57±0.05	0.48±0.06	1749.0±0.5	0.518	0.28±0.04	0.14±0.04
1277.34±0.08	0.402	0.056±0.016	0.04±0.01	1797.4±0.3	0.533	0.073±0.023	
1317.14±0.07	0.403	0.71±0.12	0.65±0.08	1799.75±0.09	0.533	1.15±0.16	0.82±0.23 (2)
1328.93±0.07	0.509	0.54±0.09	0.29±0.05	1841.5±0.5	0.419	0.153±0.018	0.09±0.02
1364.08±0.07	0.417	0.85±0.08 (2)	0.66±0.06	1898.1±0.5	0.482	0.021±0.007	0.03±0.01
1365.8±0.2	0.417		0.03±0.01	1900.0±0.5	0.450	0.008±0.006	0.02±0.01
1381.60±0.07	0.503	4.6±0.4	3.40±0.50	1907.4±0.5	0.481	0.30±0.03	
1388.36±0.07	0.480	1.83±0.16 (2)	2.00±0.40	1908.5±0.4	0.481	0.47±0.17	0.31±0.04
1388.6±0.3	0.480		0.01±0.01	1963.7±0.5	0.480	0.159±0.023	
1457.0±0.2	0.416	0.166±0.016	0.13±0.03	1969.0±0.5	0.468	0.54±0.10	0.43±0.05
1502.12±0.08	0.480	0.067±0.007	0.05±0.01	1977.4±0.6	0.464	0.52±0.07	0.55±0.11
1519.7±0.2	0.484	1.24±0.13	0.59±0.14				

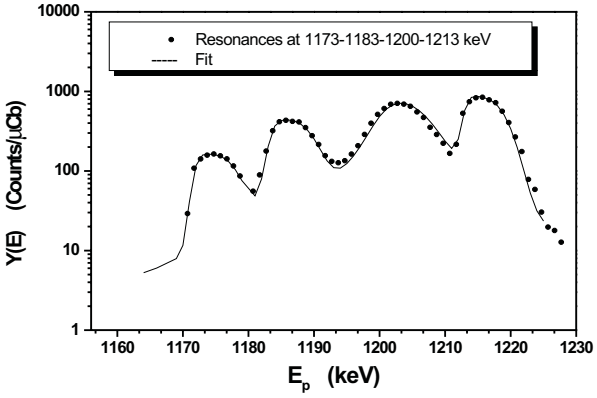

Fig. 5. Excitation function in the energy range E_p=1170-1230 keV. The solid line is the result of the fit

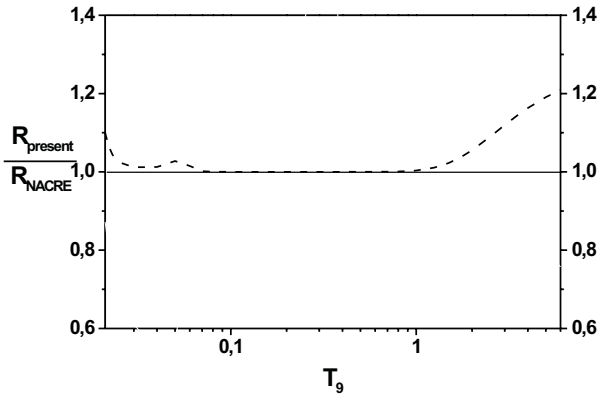

Fig. 6. Ratio of the present reaction rate to the one from NACRE compilation

In many cases, the fitting procedure was applied also to thick target measurements in order to check the validity of the results. In Table 2 all results for the 47 resonances are listed. The notation (2) after an $\omega\gamma$ quotation stands for the total strength of doublets which can not be separated. In the same table the adopted values from the NACRE compilation are also displayed.

4 Conclusions

Forty-seven resonances have been measured from E_p=800 to 2000 keV in a systematic and consistent manner. The reported values are free of gamma ray angular distribution effects and are based on a uniform and self-consistent efficiency correction method. For many of the resonances there is an excellent agreement between the measured resonance strengths and the adopted values in the NACRE compilation [1]. However for some resonances, discrepancies exist, mostly for resonances where the number of previously reported and compiled measurements is small or the weighted average value adopted is dictated by one particular value accompanied by an abnormally low error. For three resonances at E_p=1797, 1900 and 1964 keV, strengths are reported for the first time.

The presently measured resonance strengths are expected to influence the astrophysical reaction rate in the temperature range of T_9=1.3-6 as compared with the NACRE compilation. In order to quantify this influence, the reaction rate has been recalculated as prescribed in the NACRE compilation [1]. Above E_p=800 keV the presently reported resonance strengths have been used, while for E_p below 800 keV, the NACRE adopted values have been used. The ratio of the present reaction rate to the NACRE one is shown in Fig. 6. The ratio increases significantly above T_9=2 and at T_9=6 the present reaction rate is about 20% higher than the NACRE compilation. However, a recompilation of the resonance strengths by addition of the present values to the compiled ones by NACRE, will result in a smoothing of this effect and the maximum deviation at T_9=6 from the recommended NACRE reaction rate will not exceed +5%. This is less than the quoted error in the compilation.

References

1. **N**uclear **A**strophysics **C**ompilation of **RE**action Rates (**NACRE**), C. Angulo, M. Arnould, and M. Rayet, P. Descouvemont, D. Baye, and C. Leclerq-Willain, A. Coc, S. Barhoumi, and P. Auger, C. Rolfs, R. Kunz, J.W. Hammer, and A. Mayer, T. Paradellis, S. Kossionides, C. Chronidou, and K. Spyrou, S. Degl'Innocenti, G. Fiorentini, B. Ricci, and S. Zavaratelli, C. Providencia, H. Walters, and J. Soares, C. Crama, J. Rahighi, A. Shotter, and M. Lamehi Rachti, Nucl. Phys. **A656**, 3 (1999)
2. K. Spyrou, C. Chronidou, S. Harissopulos, S. Kossionides, T. Paradellis, Z. Phys. **A357**, 283 (1997)
3. GEANT - Detector description and Simulation Tool: CERN Geneva, 1993
4. P. M. Endt et al, Nucl. Phys. **A510**, 209 (1990)
5. P. M. Endt, Nucl. Phys. **A521**, 1 (1990)
6. E. F. Gibbons et al, Phys. Rev. **172**, 1004 (1968)
7. M. A. Meyer et al, Nucl. Phys. **A136**, 663 (1969)
8. M. A. Meyer et al, Nucl. Phys. **A144**, 261 (1970)
9. S. T. Lam et al, Can. J. Phys. **49**, 685 (1971)
10. M. A. Meyer, I. Venter, and D. Reitman, Nucl. Phys. **A250**, 235 (1975)
11. M. J. Dalmas, Can. J. Phys. **56**, 917 (1978)
12. C. Rolfs, W.S. Rodney, *Cauldrons in the Cosmos* (Chicago: University of Chicago Press, 1988)
13. H.H. Andersen and J.F. Ziegler,*Hydrogen Stopping Powers and Ranges in All Elements*, Volume 3, Pergamon Press, New York (1997)
14. G. Deconninck, *Introduction to Radioanalytical Physics* (Budapest: Akademiai Kiado, 1978)